# Kinetic simulation of flameless burners with methane/hydrogen blended fuel

Salavati-Zadeh, Ali; Esfahanian, Vahid; Nourani Najafi, Seyyed Bahram; Saeed, Hossein; Mohammadi, Mobin

*Published in:*
International Journal of Hydrogen Energy

*DOI:*
10.1016/j.ijhydene.2017.11.149



*Publication date:*
2018

Available online at www.sciencedirect.com

ScienceDirect

journal homepage: www.elsevier.com/locate/he

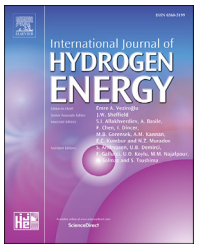

# Kinetic simulation of flameless burners with methane/hydrogen blended fuel: Effects of molecular diffusion and Schmidt number☆

Ali Salavati-Zadeh [a], Vahid Esfahanian [a,b,*], Seyyed Bahram Nourani Najafi [c], Hossein Saeed [b], Mobin Mohammadi [b]

[a] Vehicle, Fuel and Environment Research Institute (VFERI), University of Tehran, Iran
[b] School of Mechanical Engineering, Faculty of Engineering, University of Tehran, Iran
[c] Energy and Sustainability Research Institute Groningen (ESRIG), University of Groningen, The Netherlands

ARTICLE INFO

*Article history:*
Received 30 August 2017
Received in revised form
20 November 2017
Accepted 27 November 2017
Available online 21 December 2017

*Keywords:*
Flameless combustion
Molecular diffusion
Schmidt number

ABSTRACT

The newly developed concept of MILD combustion has paved the way through achievement of high thermal efficiencies with low levels of pollutants and greenhouse gases. High fidelity numerical models play key role in design and optimization of these burners. The present research aims to assess the effect of molecular diffusion and deviations in the amount of different species Schmidt number on the precision of the model. To this end, a previously investigated MILD burner is opted as case-study. From the results it is evident that in contrast to conventional combustion regimes problems, the impact of the often-neglected laminar diffusion is comparable to turbulent diffusion. On the other hand, consideration of molecular diffusion in the species transport equation significantly improves the model accuracy only if proper Schmidt number for species are considered. Suitable Sutherland coefficients and Schmidt numbers for each species are found based on relevant data in the literature and reported.



## Introduction

Today, combustion of fossil fuels has antagonistic impacts on human living. While, it enhances about 80% of the world energy demand, the pollutant species and greenhouse gases (GHG hereafter) emitted from the flames are proved to be associated with several threads to human health and environment. Carbon dioxide contributes 77% of the GHG emissions with combustion accounting for 27%, making it a major contributor to global climate change. This issue, has fired the enthusiasm of researchers and engineers in new combustion technologies. In this framework, precise numerical models are indispensable to meet the rapid responses required of regulatory agenda with feasible cost.

Preheating the reactants by the hot flue gases is proved to be a promising method to improve the combustion efficiency. This method has roots in the concept of "large excess enthalpy combustion" which was introduced in the early 1970s [1,2] and has paved the way for introduction of moderate or intense

☆ This paper was presented at the IEEES-9 conference, Split, Croatia, 14–17 May 2017.

* *Corresponding author*. Vehicle, Fuel and Environment Research Institute (VFERI), University of Tehran, Iran.
E-mail addresses: alisalavati@ut.ac.ir (A. Salavati-Zadeh), evahid@ut.ac.ir (V. Esfahanian), s.b.nourani.najafi@rug.nl (S.B. Nourani Najafi), hsaeed@ut.ac.ir (H. Saeed), mobin_mohammadi92@yahoo.com (M. Mohammadi).

https://doi.org/10.1016/j.ijhydene.2017.11.149
0360-3199/

**Nomenclature**

| | |
|---|---|
| $A$ | Sutherland relation parameter |
| $C$ | Diffusion coefficient |
| $h$ | Enthalpy |
| $k$ | Turbulent kinetic energy |
| $p$ | Static pressure |
| $R$ | Reynolds stress tensor |
| S | Source term for species conservation equation |
| Sc | Schmidt number |
| $t$ | Time |
| $T$ | Temperature |
| $u$ | Velocity |
| Y | Mass fraction |

*Greek letters*

| | |
|---|---|
| $\varepsilon$ | Turbulent dissipation rate |
| $\mu$ | Dynamic (absolute) viscosity |
| $\rho$ | Density |
| $\omega$ | Source term for species conservation equation |

*Subscripts and superscripts*

| | |
|---|---|
| i, j, k | Pertinent to coordinate system |
| l | Pertinent to lth specie |
| M | Pertinent to molecular |
| S | Pertinent to sutherland |
| T | Pertinent to turbulent |

low-oxygen dilution (MILD hereafter) combustion also known as flameless combustion [3]. Nevertheless, considering its different characteristics, this regime is known with several other names, some of which are: High Temperature Air Combustion or HiTAC [4], Colorless Combustion [5], invisible flame [6], High Temperature Combustion Technology or HiCOT [3], and the green flame [7]. Beside high efficiency, excellent combustion stability, uniform temperature distribution and extremely low emissions of NOx [8,9] are known as other beneficial features to flameless combustion regime. This last feature made researches i.e., Mardani and Tabejamaat [10], Li et al. [11] and Galletti et al. [12], to perform experimental and kinetic studies on formation of nitrogen oxides.

With the oxygen dilution range of 3–13% and reactant temperature always higher than the auto ignition temperature, the flameless combustion characteristics differ greatly from normal combustion. Therefore, many researches have addressed characteristics of flameless burners. Aminian et al. [13] numerically investigated the structure of a flameless burner with three different fractions of oxygen in hot coflow air jet using steady state Reynolds-Averaged Navier-Stokes (RANS hereafter) approach coupled with the Eddy Dissipation Concept (EDC hereafter) [14–16] for treating chemistry-turbulence interaction. Four variants of the well-known $k-\varepsilon$ model, i.e., standard, modified, realizable and RNG, and three different reduced kinetic schemes, i.e., DRM-19, DRM-22 and KEE-58, were utilized. The results indicate better performance of the KEE-58 mechanism in comparison with other schemes. Nevertheless, a large over-prediction of temperature and chemical species, except for oxygen molecule, at downstream was assessed for all flames, particularly for the flame with the lowest amount of oxygen in the hot coflow stream, i.e., 3%. It was also indicated that localized extinction did not contribute in the overprediction, which was thought to be due to turbulence-chemistry interaction model employed, whose importance was previously emphasized by Parente et al. [17] and Mardani et al. [18]. Also, for MILD regime, higher residence time in the fine structures for MILD combustion was indicated camparing with conventional combustion. Before that, Aminian et al. [19] and Frassoldati et al. [20] have shown the importance of implementing boundary conditions in utilizing coupled modified $k-\varepsilon$ model and EDC with reduced chemical mechanisms to simulate the MILD burners using $CH_4-H_2$ blends. In addition, MILD burners whose fuel jet are enriched with hydrogen have been subject of numerous other investigations. Mardani and Tabejamaat [21] studied the influence of hydrogen amount used to enrich methane fuel for burning under MILD conditions. In this research, which have employed modified $k-\varepsilon$ model coupled with EDC, improvements in mixing, and increase in mixture ignitability, flame entrainment, reaction intensities and rate of heat release with increase in the amount of hydrogen was assessed. Later, Afarin and Tabejamaat [22] utilized Large Eddy Simulation (LES) to study the effect of hydrogen enrichment and to show the increase in flame thickness and decrease in hydroxide oscillations in presence of hydrogen. In addition, in other research [23] they used LES to investigate the impact of fuel inlet turbulence intensity on the MILD flame structure and weakening of the combustion zone. In these two researches, the turbulence-chemistry interactions were modelled under the light of utilizing a modified version of EDC which is commonly referred as Partially Stirred Reactor (PaSR hereafter) model [24]. It is worth considering that turbulent transport, rooted in velocity fluctuations that act to efficiently transport momentum, heat, and species concentration, is significantly more effective that molecular diffusion [25]. The turbulence high rate of diffusivity caused molecular diffusion be neglected in many researches that deal with conventional turbulent combustion problems. Similarly, in the researches mentioned above, only the turbulent diffusion is considered. The effect of molecular diffusion was compared with that of turbulent diffusion in the flameless combustion regime by Mardani et al. [26] and the outcomes of using two different methodologies for considering molecular diffusion, i.e., bimolecular and multicomponent, were assessed. This research proved the importance of considering molecular diffusion taking the special characteristics of this regime into account.

The present research aims to investigate the influence of molecular diffusion on the validity of numerical simulation results for a burner working at flameless conditions for different inlet configurations. To accomplish this, a flameless burner is simulated with two different strategies; in the first strategy, the molecular diffusion is neglected, whereas in the second strategy, it is taken into account in the formulation. Also, two different methodologies are used for implementing the latter strategy to observe the impact of considering variations in Schmidt number of each specie on the fidelity of the results. The results are compared with each other and their deviation from the experimental observations, which has been reported by Dally et al. [27], are also assessed. Sutherland

approach is used to model the molecular diffusion. The list of Sutherland parameters and Schmidt numbers used are also provided in the manuscript.

## Modeling strategy

To overcome the problem of introduction of additional unknowns (Reynolds stresses) to the momentum equation, i.e.,

$$\rho\left(\frac{\partial \overline{u}_i}{\partial t}+\overline{u}_k\frac{\partial \overline{u}_i}{\partial x_k}\right)=-\frac{\partial \overline{p}}{\partial x_i}+\frac{\partial}{\partial x_j}\left(\overline{\mu}\frac{\partial \overline{u}_i}{\partial x_j}\right)+\frac{\partial R_{ij}}{\partial x_j} \quad (1)$$

In Eq. (1) the bar indicate the mean values for velocity components and pressure. Also, the average amount for dynamic viscosity is considered. To close the system of governing equations, the Reynolds stresses are modelled using an eddy (or turbulent) viscosity, $\mu_T$, which is calculated based on the turbulent model employed. In the present research, the turbulent flow field is simulated using $k-\varepsilon$ RANS approach, which solves the transport equations for $k$ and $\varepsilon$:

$$\mu_T=f\left(\frac{\rho k^2}{\varepsilon}\right) \quad (2)$$

This robust modeling technique could be considered as one of the most widely used turbulence models. Nevertheless, it may perform poorly for flows where large curvature of streamlines and strong curvatures are present [28], which are not present in the physical domain. The modifications made in the formulation will be discussed in section 2.2.

The PaSR technique is employed to model the turbulence-chemistry interaction. The chemistry of the combustion is also modelled using KEE-58 reduced scheme which consists of 17 species and 58 reversible primary reactions related to $C_1$ [29]. The burner is simulated using axisymmetric assumption. All the simulations are carried out using OpenFOAM v. 3.0 software package.

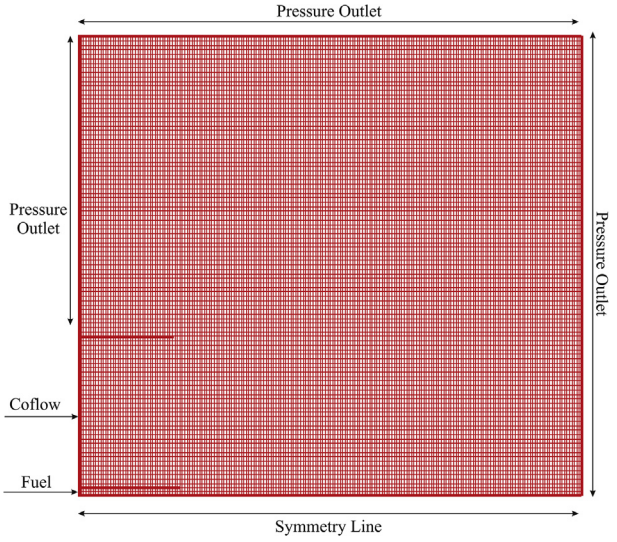


**Fig. 1 – (Color online) Computational domain. (For interpretation of the references to color/colour in this figure legend, the reader is referred to the Web version of this article.)**

**Table 1 – Sutherland coefficients used for different species.**

| Species | $A_S$ | $T_S$ |
|---|---|---|
| H | $6.64e-7$ | 117.81 |
| O | $2.18e-6$ | 166.69 |
| N | $1.86e-6$ | 188.2 |
| OH | $1.62e-6$ | 273.93 |
| $H_2$ | $7.04e-7$ | 108.3 |
| $O_2$ | $1.8e-6$ | 151.03 |
| $N_2$ | $1.5e-6$ | 135.27 |
| NO | $1.65e-6$ | 147.75 |
| CO | $1.53e-6$ | 146.32 |
| $CO_2$ | $1.49e-6$ | 218.83 |
| $H_2O$ | $2.46e-6$ | 916.58 |
| $H_2O_2$ | $1.58e-6$ | 489.05 |
| $CH_4$ | $1.03e-6$ | 178.78 |

### *Case-study*

The flameless burner considered is a well-recognized benchmark of fuel-jet-in-hot-coflow burner first studied experimentally by Dally et al. [27]. This research contains detail description about the burner configuration and three sets of experiment carried out, and a summary is brought here.

The burner was consisted of three main cylindrical co-centric parts, including fuel stream situated in the center surrounded by hot air coflow and surrounding air, respectively. Taking the symmetry of the burner into account, two-dimensional steady-state simulation of the half-top of the physical domain is performed. Fig. 1 shows the computational grid used and the adopted boundary conditions. A structured non-uniform grid is utilized in a domain of $120 \times 100$ mm in the axial and radial directions from the jet exit, respectively. Since the ame is non-confined and assuming backow of ambient air, the pressure outlet condition is used.

In all the three sets of experiment, the $CH_4/H_2$ blended fuel is provided at $3.12 \times 10^{-4}$ kg/s flow rate has the temperature of 305 K has the same composition of 88% $CH_4$ and 11% $H_2$ (all the amounts are expressed as mass fractions). Also, the

**Table 2 – $Sc_M$ used for different species.**

| Species | $Sc_M$ |
|---|---|
| $H_2$ | 0.2 |
| H | 0.15 |
| O | 0.84 |
| $O_2$ | 0.84 |
| OH | 0.53 |
| $H_2O$ | 0.65 |
| $HO_2$ | 0.65 |
| $H_2O_2$ | 0.65 |
| $CH_2O$ | 0.86 |
| CH | 0.99 |
| $CH_2$ | 0.99 |
| $N_2$ | 0.87 |
| $CH_3$ | 0.99 |
| $CH_4$ | 0.99 |
| CO | 0.86 |
| $CO_2$ | 0.98 |
| HCO | 0.86 |

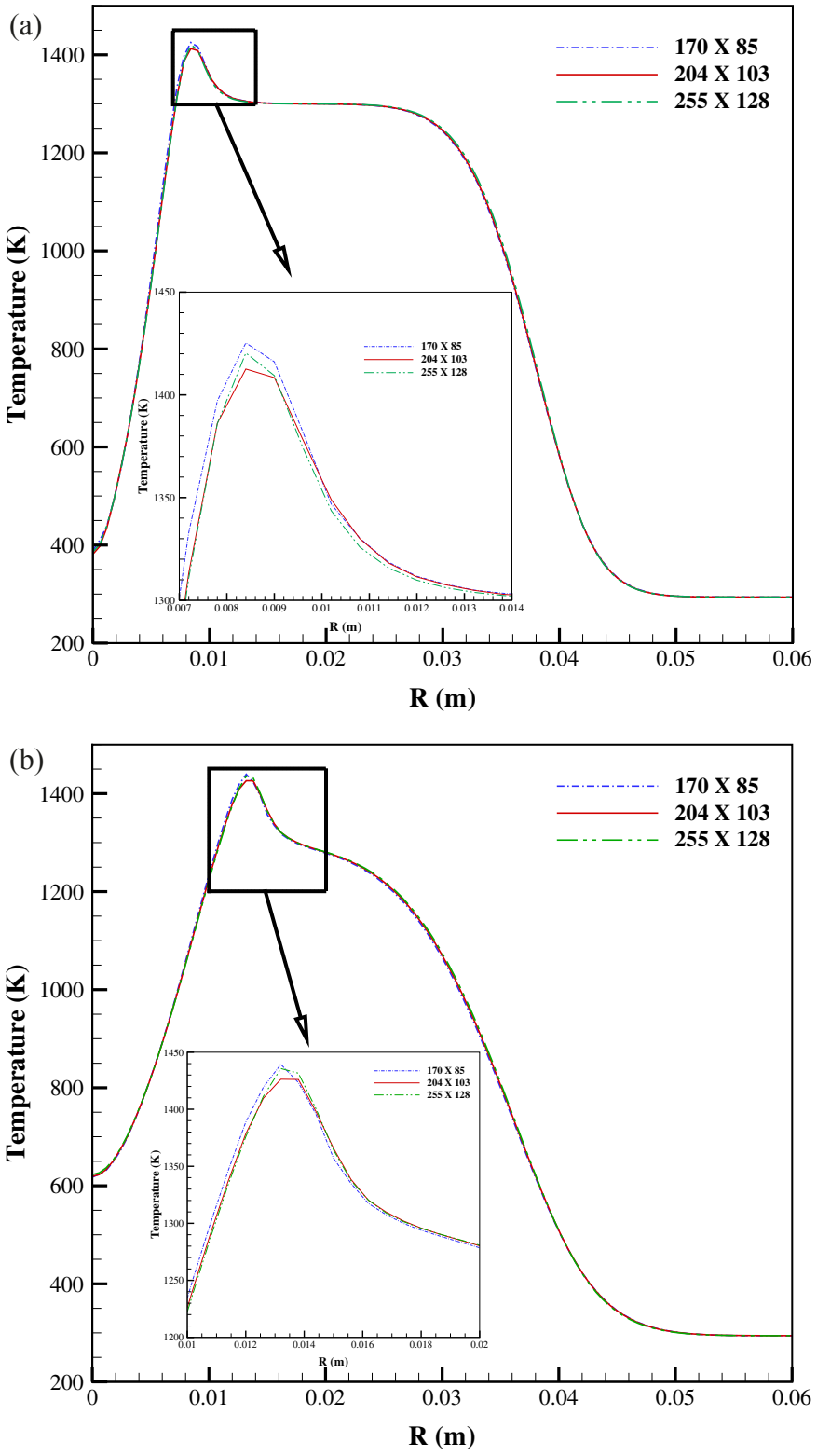


**Fig. 2 – (Color online) Comparison of the simulation results for three different grids for axial distance of (a) 30 mm; (b) 60 mm. (For interpretation of the references to color/colour in this figure legend, the reader is referred to the Web version of this article.)**

surrounding air in the tunnel contains 23.2% $O_2$, and is blown at the speed of 3.2 m/s, and temperature of 294 K. In addition, the hot oxidant coflow has the same temperature of 1300 K and flows in constant speed of 3.2 m/s in all the experiments conducted. Nevertheless, the experiments differ in the amount of oxygen which equals 3% in the first (HM1), 6% in the second (HM2) and 9% in the third setup (HM3).

### *Simulation procedure*

As mentioned earlier, the simulations are performed utilizing OpenFOAM v. 3.0 software. The species transport equation in a turbulent flow field, i.e.,

$$\frac{\partial \rho Y_l}{\partial t} + \vec{\nabla} \cdot \rho \vec{u} - \vec{\nabla} C_{l_T} \vec{\nabla} Y_l = S_l \tag{3}$$

is therefore modified to take the molecular diffusion effects into account, i.e.,

$$\frac{\partial \rho Y_l}{\partial t} + \vec{\nabla} \cdot \rho \vec{u} - \vec{\nabla} C_{l_T} \vec{\nabla} Y_l - \vec{\nabla} C_{l_M} \vec{\nabla} Y_l = S_l \tag{4}$$

where $Y_l$ is the mass fraction of $l$th species, $C_l$ is its diffusion coefficient and subscripts T and M denote turbulent and molecular diffusion, respectively. In Eqs. (3) and (4), the source term S in the right-hand side denotes the rate of production or destruction of $l$th specie, found from chemical scheme. From the definition of Schmidt number, Sc, we have:

$$C_{l_{T,M}} = \frac{\mu_{l_{T,M}}}{\rho \cdot Sc_{l_{T,M}}} \tag{5}$$

where $\mu_l$ is the dynamic (absolute) viscosity. Sutherland Formula, i.e.,

$$\mu_l = \frac{A_{S_l}\sqrt{T}}{1 + \frac{T_{S_l}}{T}} \tag{6}$$

is utilized to find the dynamic viscosity to be employed in Eq. (5). In Eq. (6), the parameters $A_S$ and $T_S$ are calculated using available data in the literature, e.g., the research of McBride et al. [30], for dynamic viscosity in 298 K and 1500 K. The achieved sutherland coefficients are brought in Table 1. The continuity, momentum and species transport equations are to be solved along with the energy equation for reactive flows, i.e.,

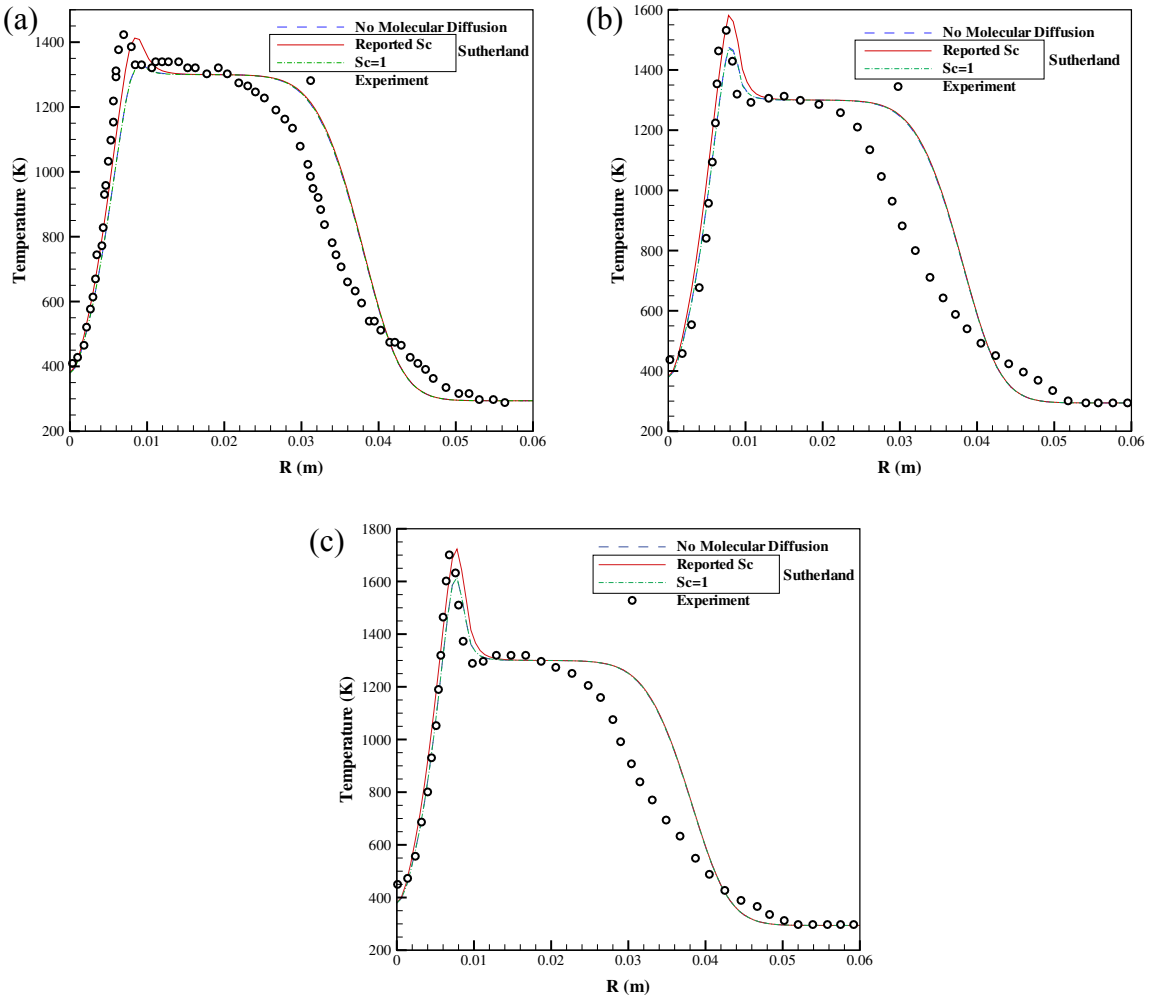


**Fig. 3 – (Color online) Comparison of experimental and numerical results for temperature at axial distance of 30 mm for (a) HM1; (b) HM2; and (c) HM3. (For interpretation of the references to color/colour in this figure legend, the reader is referred to the Web version of this article.)**

$$\frac{\partial}{\partial t}(\bar{\rho}\tilde{h}) + \frac{\partial}{\partial x_i}(\bar{\rho}u_i\tilde{h}) = \frac{Dp}{Dt} + \frac{\partial}{\partial x_i}\left(\frac{\bar{\mu}}{Pr} + \frac{\bar{\mu}_T}{Pr_T}\right)\frac{\partial h}{\partial x_i} + \omega \quad (7)$$

to obtain the results. In Eq. (7), $\omega$ is considered to be the heat source.

The turbulent Schmidt number for all species, i.e., $Sc_{l_T}$ is set to be constant and equal to 1.0. Two different strategies are taken into account in the present research for consideration of molecular diffusion. In the first strategy, the Schmidt number for molecular diffusion of lth specie, i.e., $Sc_{l_M}$ is set to be constant equal to 1.0. in the second strategy, the available data in the literature for $Sc_{l_M}$, e.g., Ref. [31], is utilized. It should be mentioned that in both strategies the dynamic viscosity is calculated employing sutherland formula as described previously. In addition, for both dynamic viscosity and $Sc_{l_M}$, if data is not available for a specie, the data for another specie with the closest molecular structure and mass are employed. The $Sc_{l_M}$ used for the species present in the mechanism, are brought in Table 2. The simulation results are then compared with the sequels of neglecting molecular diffusion in the simulation process.

### Grid study

Three different grid sizes are brought under study and the simulation results are compared. In the simulations, the molecular diffusion are taken into account in the simulations using the reported Schmidt numbers. The results for temperature at axial distances of 30 and 60 mm from the nozzle are illustrated in Fig. 2(a) and (b). All the results are reported for HM1 flame. From the results it can be seen that while the results obtained by the 170 × 85 mesh shows slight difference from the two other grids, despite little discrepancy at the point of maximum temperature which does not exceeds 0.8%, the results from the 204 × 103 and 255 × 128 grids agree well, and the 204 × 103 grid is opted in this research.

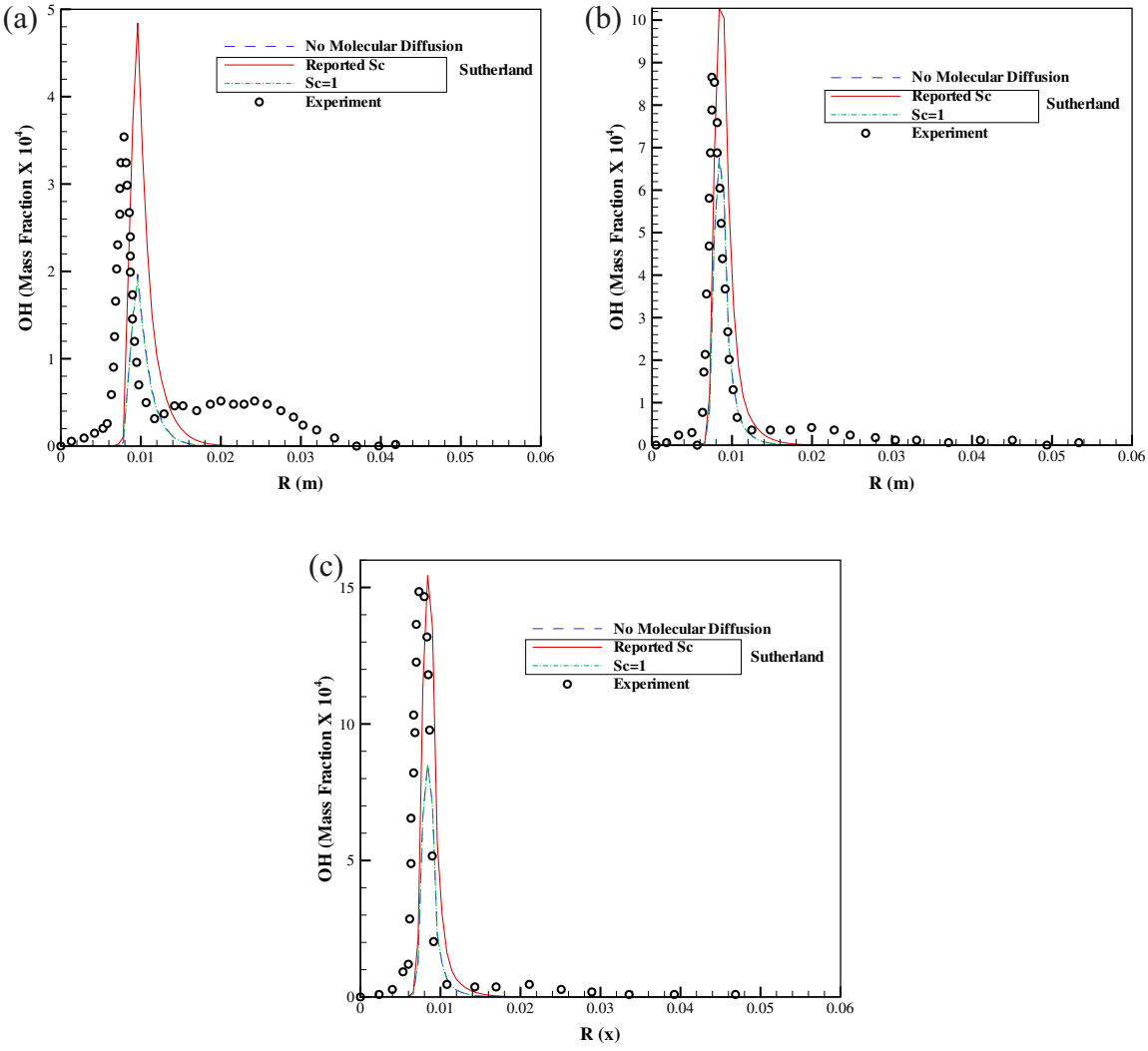


**Fig. 4 – (Color online) Comparison of experimental and numerical results for OH profile at axial distance of 30 mm for (a) HM1; (b) HM2; and (c) HM3. (For interpretation of the references to color/colour in this figure legend, the reader is referred to the Web version of this article.)**

## Results and discussion

The temperature profiles for axial distance of 30 mm are depicted in Fig. 3. By a careful assessment on the results, two very important points could be indicated. First, the simulation results achieved by neglecting the molecular diffusion are very close to those considering constant Sc for all of the species. This proves the crucial role of Schmidt number. Second, as the amount of oxygen molecule in the hot coflow jet increases, the impact of considering molecular diffusion on accuracy of the results seems to vanish and the results of the model neglecting molecular diffusion become more accurate. Meanwhile, the results of all models seem to be more precise by increasing the amount of molecular oxygen in the hot coflow. These observations seem to be due to the fact that the conventional combustion regime will begin to dominate the field when the amount of oxygen increase. This is consistent with the findings reported by Mardani et al. [26]. In spite of this, for lower amounts of oxygen, consideration of molecular diffusion with proper Sc for each species, improves the accuracy for about 6%.

Observing the results for OH profile at distance of 30 mm (Fig. 4) reveals that the model performances when neglecting molecular diffusion and taking it into account considering specific Schmidt number of each specie are quite different. Considering molecular diffusion by employing Sutherlands law and the data for Sc overpredicts the amount of OH, whereas neglecting the molecular diffusion or taking the Sc equal to 1 for all species results in underprediction in the amount of OH. In addition, similar to the results for temperature, if the Sc is set to be equal to 1, the model results are similar to those obtained neglecting molecular diffusion. On the other hand, consideration of molecular diffusion with specific Sc causes the root mean square of the errors between experimental observations and numerical findings be reduced by nearly 60%. It is worth mentioning that increase in the amount of oxygen in the hot coflow stream ends in better accuracy of the outcomes of all the strategies. This is

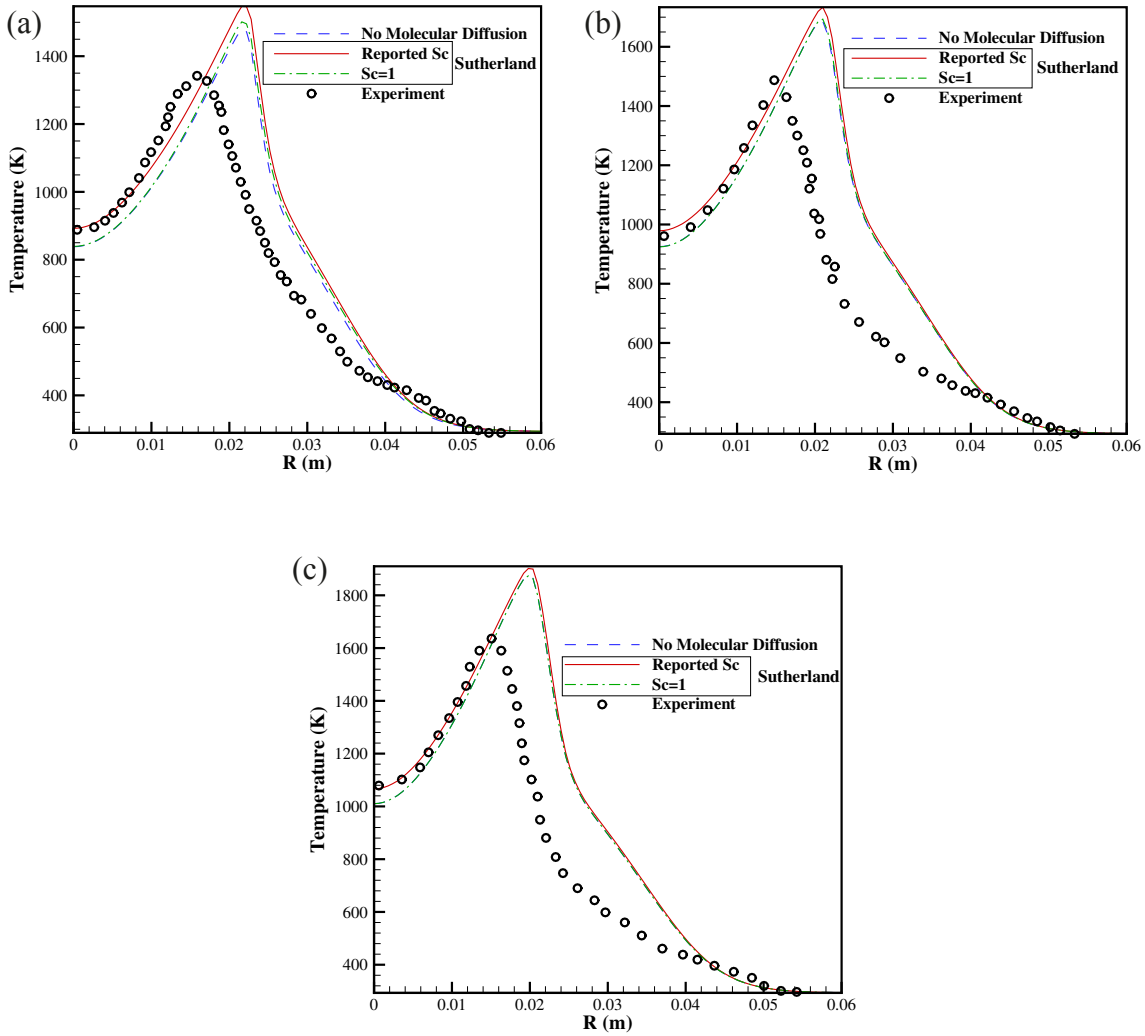


**Fig. 5 – (Color online) Comparison of experimental and numerical results for temperature at axial distance of 120 mm for (a) HM1; (b) HM2; and (c) HM3. (For interpretation of the references to color/colour in this figure legend, the reader is referred to the Web version of this article.)**

consistent with the achievements when studying temperature profile (Fig. 3).

To assess the impact of spatial position of section under study on the importance of molecular diffusion in accuracy of the results, the obtained outcomes for temperature profiles at axial distance of 120 mm from the fuel inlet for all the flames are depicted in Fig. 5. The results indicate that as the axial distance of the studied section from the fuel inlet is increased, the importance of considering molecular diffusion vanishes and the results obtained employing different strategies become more close. The results obtained by all simulation strategies also collapse into similar values as we enter the domain of surrounding air, where no reaction and mixing occurs and the turbulence governs the flow field. In spite of this, by comparing Figs. 3 and 5, it is concluded that by going far from the fuel inlet the accuracy of the results also decays.

The contours for temperature, OH and $CH_4$ concentrations distributions inside the burner are illustrated in Figs. 6–8,

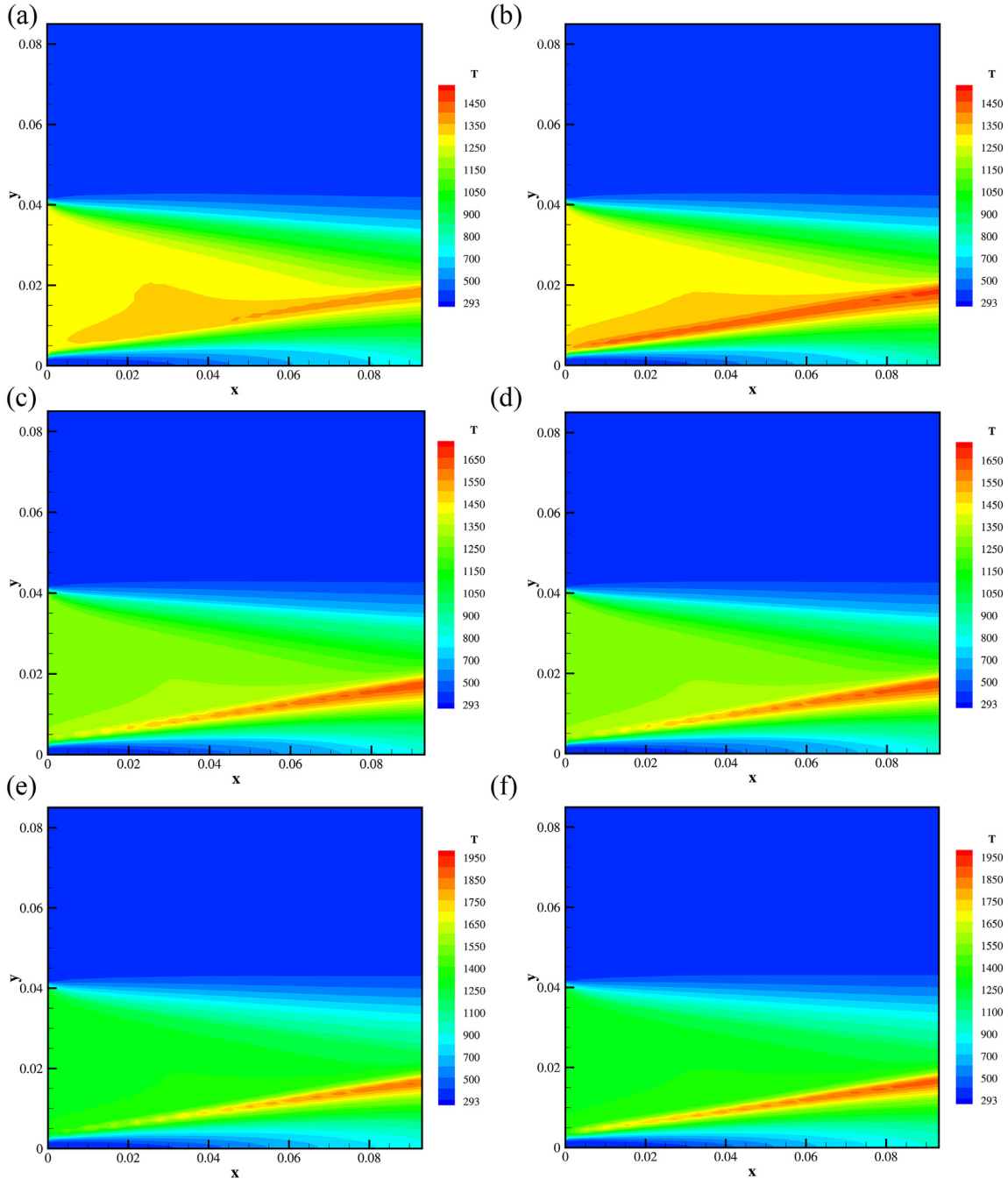


**Fig. 6 – (Color online) Temperature results yielded for (a) & (b) HM1; (c) & (d) HM2; (e) & (f) HM3. The results obtained neglecting diffusion are depicted at the left whereas the results on the right are found considering diffusion and species specific Sc. (For interpretation of the references to color/colour in this figure legend, the reader is referred to the Web version of this article.)**

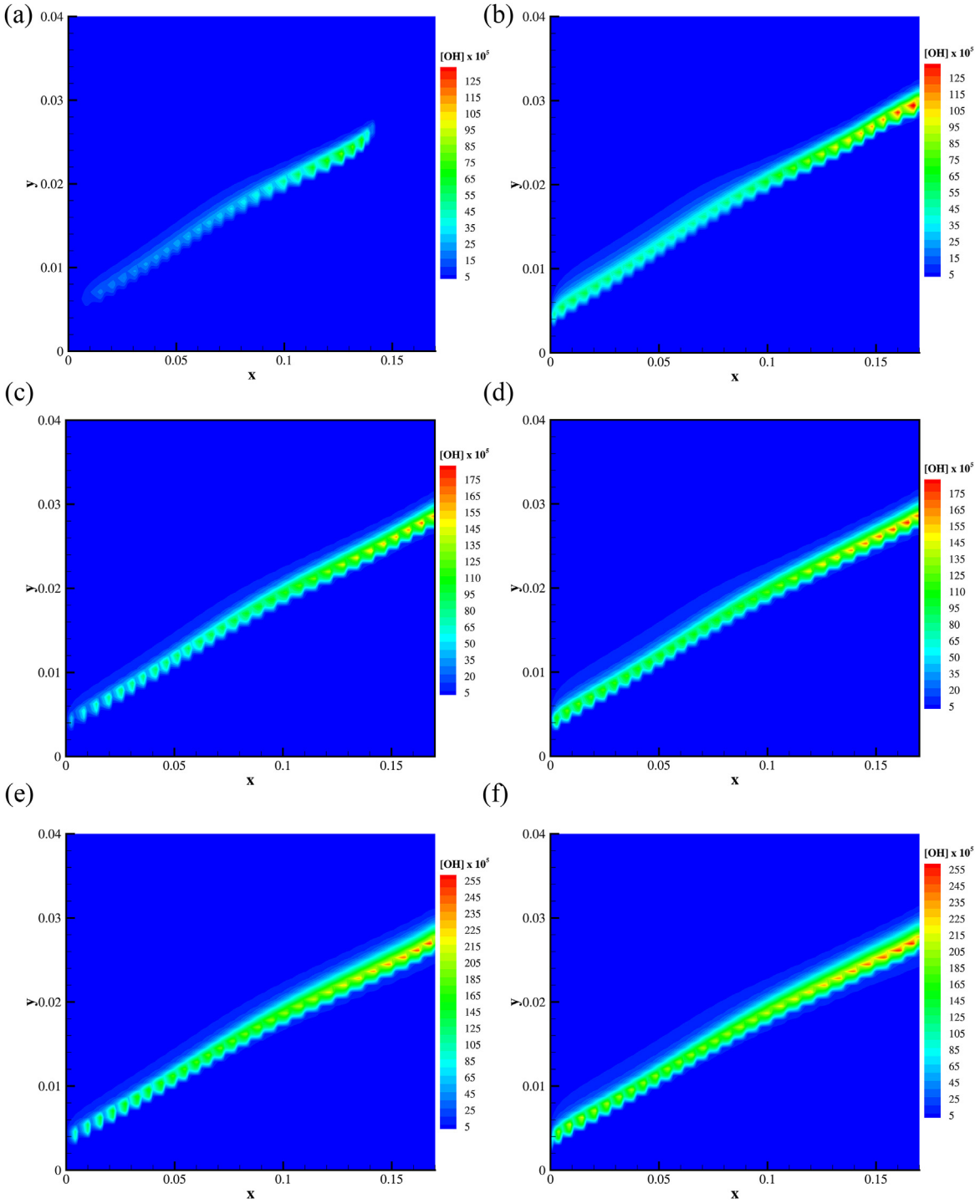


**Fig. 7 – (Color online) OH concentration results yielded for (a) & (b) HM1; (c) & (d) HM2; (e) & (f) HM3. The results obtained neglecting diffusion are depicted at the left whereas the results on the right are found considering diffusion and species specific Sc. (For interpretation of the references to color/colour in this figure legend, the reader is referred to the Web version of this article.)**

respectively. The results obtained neglecting molecular diffusion are brought on the left side, i.e., Fig. 6(a), (c) and (e) for temperature distribution contours, Fig. 7(a), (c) and (e) for OH concentration contours and Fig. 8(a), (c) and (e) for $CH_4$ concentration contours. On the other hand, the outcomes of taking molecular diffusion into account with specific Schmidt number for each specie is brought on the right side, i.e., Fig. 6(b), (d) and (f) for temperature distribution contours, Fig. 7(b), (d) and (f) for OH concentration contours and Fig. 8(b), (d) and (f) for $CH_4$ concentration contours. From Fig. 6 it could be indicated that the flame lift-off could be simulated while neglecting or considering molecular diffusion into account.

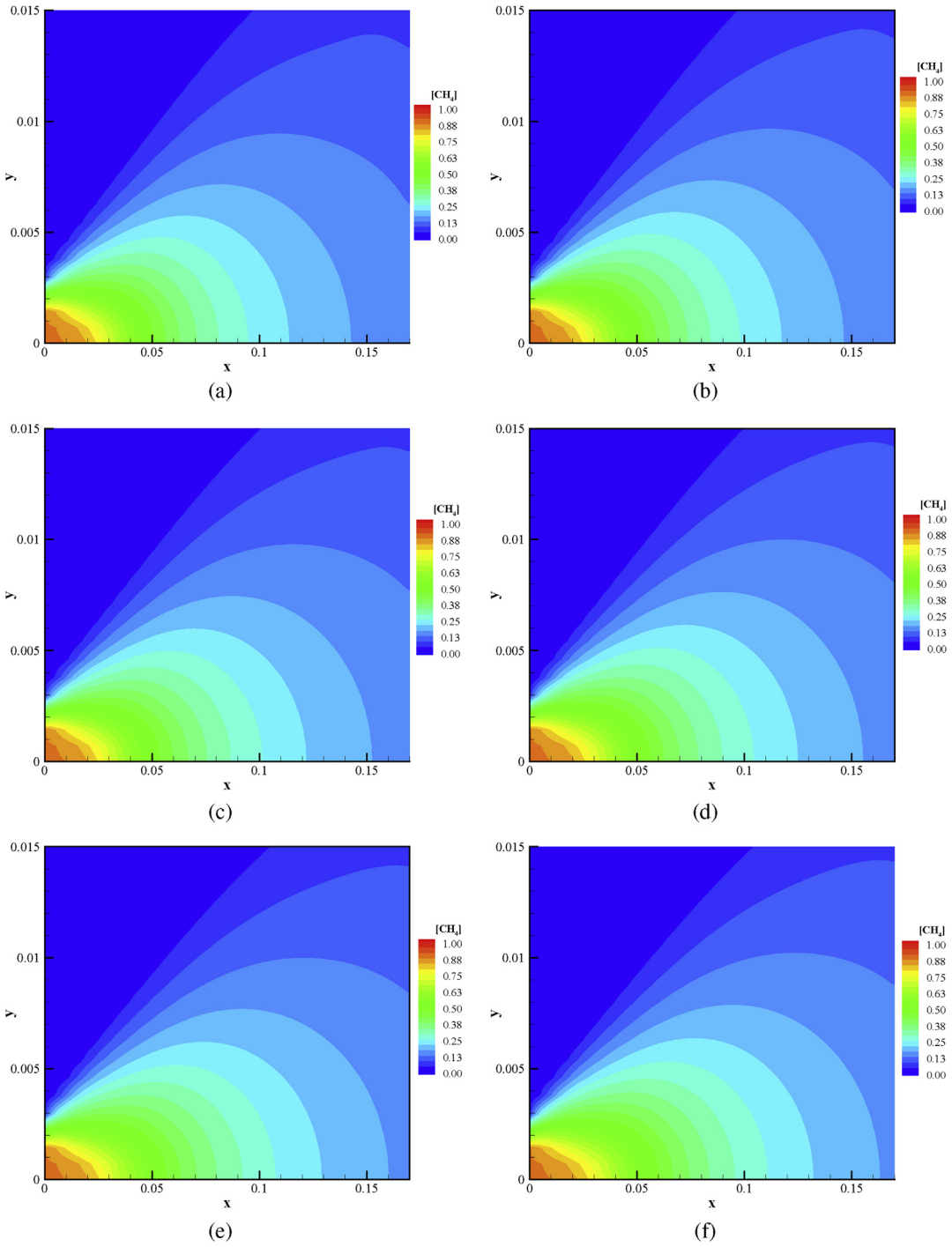


**Fig. 8 – (Color online) $CH_4$ concentration results yielded for (a) & (b) HM1; (c) & (d) HM2; (e) & (f) HM3. The results obtained neglecting diffusion are depicted at the left whereas the results on the right are found considering diffusion and species specific Sc. (For interpretation of the references to color/colour in this figure legend, the reader is referred to the Web version of this article.)**

On the other hand, as the amount of oxygen in the hot coflow jet increases, the patterns become more similar. This also applies for OH and $CH_4$ concentration distribution contours, i.e., Figs. 7 and 8. This could also be interpreted taking the role of conventional combustion regime with increase in the amount of oxygen into account.

## Conclusion

The effect of molecular diffusion and deviations in the amount of different species Schmidt number on the accuracy of the model for a flameless burner is studied. The burner

simulated has previously been investigated experimentally by Dally et al. [27]. The simulations are carried out using OpenFOAM v. 3.0 solver package. The RNG $k-\varepsilon$ model is employed for simulation of turbulence flow field, chemistry-turbulence interaction is simulated using Partially Stirred Reactor (PaSR) model the KEE-58 reduced chemical scheme is utilized to model the combustion chemistry. The following results were obtained:

1. Considering the effect of molecular diffusion has no significant effect on the results, unless the specific Schmidt numbers for all species are considered.
2. Neglecting the molecular diffusion term will cause the model to underpredict the amount of OH produced, whereas bringing molecular diffusion into account will lead to overprediction of the result.
3. Considering the molecular diffusion with proper Schmidt number for each of the species improves the accuracy of the temperature results by about 6% near the fuel inlet plane.
4. In numerical simulation of OH radical production, considering the molecular diffusion with proper Schmidt number for each of the species reduces the amount of discrepancy between numerical simulation results and experimental observations by about 60% near the fuel inlet plane.
5. The influence of molecular diffusion decays as we go far from the fuel inlet. In other words, the results of the two approaches, neglecting and bringing the molecular diffusion into account collapse on the same value as we go far from the fuel nozzle.
6. The flame lift-off could be observed in simulation results when both strategies for simulation of a flameless burner is utilized.

## Acknowledgement

This research was supported by the Vehicle, Fuel and Environment Research Institute (VFERI), University of Tehran. The authors would also like to express their thanks to Dr. H. Pasdarshahri, Tarbiat Modares University, Iran.

## REFERENCES

[1] Weinberg FJ. Combustion temperatures: the future? Nature 1971;233(5317):239–41. https://doi.org/10.1038/233239a0. http://www.nature.com/doifinder/10.1038/233239a0.

[2] Hardesty DR, Weinberg FJ. Burners producing large excess enthalpies. Combust Sci Technol 1973;8(5–6):201–14. https://doi.org/10.1080/00102207308946644. http://www.tandfonline.com/doi/abs/10.1080/00102207308946644.

[3] Cavaliere A, de Joannon M. Mild combustion. Prog Energy Combust Sci 2004;30(4):329–66. https://doi.org/10.1016/j.pecs.2004.02.003. http://linkinghub.elsevier.com/retrieve/pii/S0360128504000127.

[4] Katsuki M, Hasegawa T. The science and technology of combustion in highly preheated air. Symposium Int Combust 1998;27(2):3135–46. https://doi.org/10.1016/S0082-0784(98)80176-8. http://linkinghub.elsevier.com/retrieve/pii/S0082078498801768.

[5] Gupta AK, Bolz S, Hasegawa T. Effect of air preheat temperature and oxygen concentration on flame structure and emission. J Energy Resour Technol 1999;121(3):209. https://doi.org/10.1115/1.2795984. http://energyresources.asmedigitalcollection.asme.org/article.aspx?articleid=1413851.

[6] Choi G-M, Katsuki M. Advanced low NOx combustion using highly preheated air. Energy Convers Manag 2001;42(5):639–52. https://doi.org/10.1016/S0196-8904(00)00074-1. http://linkinghub.elsevier.com/retrieve/pii/S0196890400000741.

[7] Gupta AK. Thermal characteristics of gaseous fuel flames using high temperature air. J Eng Gas Turbines Power 2004;126(1):9. https://doi.org/10.1115/1.1610009. http://gasturbinespower.asmedigitalcollection.asme.org/article.aspx?articleid=1421717.

[8] Wünning J. Flameless oxidation to reduce thermal no-formation. Prog Energy Combust Sci 1997;23(1):81–94. https://doi.org/10.1016/S0360-1285(97)00006-3. http://linkinghub.elsevier.com/retrieve/pii/S0360128597000063.

[9] Abuelnuor AAA, Wahid MA, Mohammed HA, Saat A. Flameless combustion role in the mitigation of NO $_x$ emission: a review. Int J Energy Res 2014;38(7):827–46. https://doi.org/10.1002/er.3167. doi:10.1002/er. 3167.

[10] Mardani A, Tabejamaat S. $NO_x$ Formation in $H_2$-$CH_4$ blended flame under MILD conditions. Combust Sci Technol 2012;184(7–8):995–1010. https://doi.org/10.1080/00102202.2012.663991. http://www.tandfonline.com/doi/abs/10.1080/00102202.2012.663991.

[11] Li P, Wang F, Mi J, Dally B, Mei Z, Zhang J, et al. Mechanisms of NO formation in MILD combustion of CH4/H2 fuel blends. Int J Hydrogen Energy 2014;39(33):19187–203. https://doi.org/10.1016/j.ijhydene.2014.09.050. http://linkinghub.elsevier.com/retrieve/pii/S0360319914025713.

[12] Galletti C, Ferrarotti M, Parente A, Tognotti L. Reduced NO formation models for CFD simulations of MILD combustion. Int J Hydrogen Energy 2015;40(14):4884–97. https://doi.org/10.1016/j.ijhydene.2015.01.172. http://linkinghub.elsevier.com/retrieve/pii/S0360319915002645.

[13] Aminian J, Galletti C, Shahhosseini S, Tognotti L. Numerical investigation of a MILD combustion burner: analysis of mixing field, chemical kinetics and turbulence-chemistry interaction, flow. Turbul Combust 2012;88(4):597–623. https://doi.org/10.1007/s10494-012-9386-z. http://link.springer.com/10.1007/s10494-012-9386-z.

[14] Magnussen B, Hjertager B. On mathematical modeling of turbulent combustion with special emphasis on soot formation and combustion. Symposium Int Combust 1977;16(1):719–29. https://doi.org/10.1016/S0082-0784(77)80366-4. http://linkinghub.elsevier.com/retrieve/pii/S0082078477803664.

[15] Magnussen B, Hjertager B, Olsen J, Bhaduri D. Effects of turbulent structure and local concentrations on soot formation and combustion in C2H2 diffusion flames. Symposium Int Combust 1979;17(1):1383–93. https://doi.org/10.1016/S0082-0784(79)80130-7. http://linkinghub.elsevier.com/retrieve/pii/S0082078479801307.

[16] Ertesvåg IS, Magnussen BF. The eddy dissipation turbulence energy cascade model. Combust Sci Technol 2000;159(1):213–35. https://doi.org/10.1080/00102200008935784. http://www.tandfonline.com/doi/abs/10.1080/00102200008935784.

[17] Parente A, Galletti C, Tognotti L. Effect of the combustion model and kinetic mechanism on the MILD combustion in an industrial burner fed with hydrogen enriched fuels. Int J Hydrogen Energy 2008;33(24):7553–64. https://doi.org/

10.1016/j.ijhydene.2008.09.058. http://linkinghub.elsevier.com/retrieve/pii/S0360319908011907.

[18] Mardani A, Tabejamaat S, Mohammadi MB. Numerical study of the effect of turbulence on rate of reactions in the MILD combustion regime. Combust Theory Model 2011;15(6):753–72. https://doi.org/10.1080/13647830.2011.561368. http://www.tandfonline.com/doi/abs/10.1080/13647830.2011.561368.

[19] Aminian J, Galletti C, Shahhosseini S, Tognotti L. Key modeling issues in prediction of minor species in diluted-preheated combustion conditions. Appl Therm Eng 2011;31(16):3287–300. https://doi.org/10.1016/j.applthermaleng.2011.06.007. http://linkinghub.elsevier.com/retrieve/pii/S1359431111003176.

[20] Frassoldati A, Sharma P, Cuoci A, Faravelli T, Ranzi E. Kinetic and fluid dynamics modeling of methane/hydrogen jet flames in diluted coflow. Appl Therm Eng 2010;30(4):376–83. https://doi.org/10.1016/j.applthermaleng.2009.10.001. http://linkinghub.elsevier.com/retrieve/pii/S1359431109002920.

[21] Mardani A, Tabejamaat S. Effect of hydrogen on hydrogen methane turbulent non-premixed flame under MILD condition. Int J Hydrogen Energy 2010;35(20):11324–31. https://doi.org/10.1016/j.ijhydene.2010.06.064. http://linkinghub.elsevier.com/retrieve/pii/S0360319910012401.

[22] Afarin Y, Tabejamaat S. Effect of hydrogen on H2/CH4 flame structure of MILD combustion using the LES method. Int J Hydrogen Energy 2013;38(8):3447–58. https://doi.org/10.1016/j.ijhydene.2012.12.065. http://linkinghub.elsevier.com/retrieve/pii/S0360319912027358.

[23] Afarin Y, Tabejamaat S. The effect of fuel inlet turbulence intensity on $H_2/CH_4$ flame structure of MILD combustion using the LES method. Combust Theory Model 2013;17(3):383–410. https://doi.org/10.1080/13647830.2012.742570. http://www.tandfonline.com/doi/abs/10.1080/13647830.2012.742570.

[24] Chomiak J, Karlsson A. Flame liftoff in diesel sprays. Symp Combust Proc 1996;26(2):2557–64. https://doi.org/10.1016/S0082-0784(96)80088-9. http://linkinghub.elsevier.com/retrieve/pii/S0082078496800889.

[25] Peters N. Turbulent combustion. 1st ed. Cambridge University Press; 2000.

[26] Mardani A, Tabejamaat S, Ghamari M. Numerical study of influence of molecular diffusion in the Mild combustion regime. Combust Theor Model 2010;14(5):747–74. https://doi.org/10.1080/13647830.2010.512959. http://www.tandfonline.com/doi/abs/10.1080/13647830.2010.512959.

[27] Dally B, Karpetis A, Barlow R. Structure of turbulent non-premixed jet flames in a diluted hot coflow. Proc Combust Inst 2002;29(1):1147–54. https://doi.org/10.1016/S1540-7489(02)80145-6. http://linkinghub.elsevier.com/retrieve/pii/S1540748902801456.

[28] Fox R. Computational models for turbulent reactive flows. 1st ed. Cambridge University Press; 2003.

[29] Bilger R, Stårner S, Kee R. On reduced mechanisms for methane air combustion in nonpremixed flames. Combust Flame 1990;80(2):135–49. https://doi.org/10.1016/0010-2180(90)90122-8. http://linkinghub.elsevier.com/retrieve/pii/0010218090901228.

[30] B. J. Mcbride, S. Gordon, M. A. Reno, Coefficients for calculating thermodynamic and transport properties of individual species. URL https://ntrs.nasa.gov/search.jsp?R=19940013151.

[31] Turrell G. Gas dynamics: theory and applications. 1st ed. Wiley; 1997.